Sampling the World in 3D by Airborne LIDAR – Assessing the Information Content of LIDAR Point Clouds

ANDREAS ULLRICH, Horn, Austria

ABSTRACT

Every technology in remote sensing used to retrieve 3D information from sensor data and to provide point clouds as an intermediate data product – whether based on LIDAR or imagery – only takes samples on the object's surface, with limited spatial resolution in all dimensions and with finite accuracy. The information content of a point cloud data depends explicitly on the actual distribution of the samples in 3D space.

Today's market offers a variety of LIDAR instruments for airborne laser scanning with specifications sometimes hard to conceive and sometimes even misleading. Expert knowledge is often required to estimate the performance achievable with such systems in real world applications and to assess the specification's impact on the deliverable data product.

We discuss a small subset of specified features: laser pulse repetition rate, effective measurement rate, ranging capabilities, scanner type and scan speed. We investigate the achievable distribution of the measurements on the ground for typical scenarios in airborne LIDAR data acquisition for a representative selection of state-of-the-art LIDAR instruments. In particular, interference effects in scan patterns of multi-channel-output instruments are addressed.

We also propose an alternative metric for quantifying the distribution of measurements on the ground which provides more insight than the classical points-per-square-meter metric. A figure of merit for the ground sampling quality is derived allowing the comparison between LIDAR instruments based on different technologies.

1. INTRODUCTION

Point clouds are an established intermediate data product in a wide variety of remote sensing techniques used to retrieve 3D information from sensor data, whether based on LIDAR, radar, or imagery. However, all remote sensing systems only take samples on the object's surface or sometimes volume, with limited spatial resolution in all dimensions and with finite accuracy. The information content of the acquired point cloud data depends explicitly on the actual distribution of the samples in 3D space.

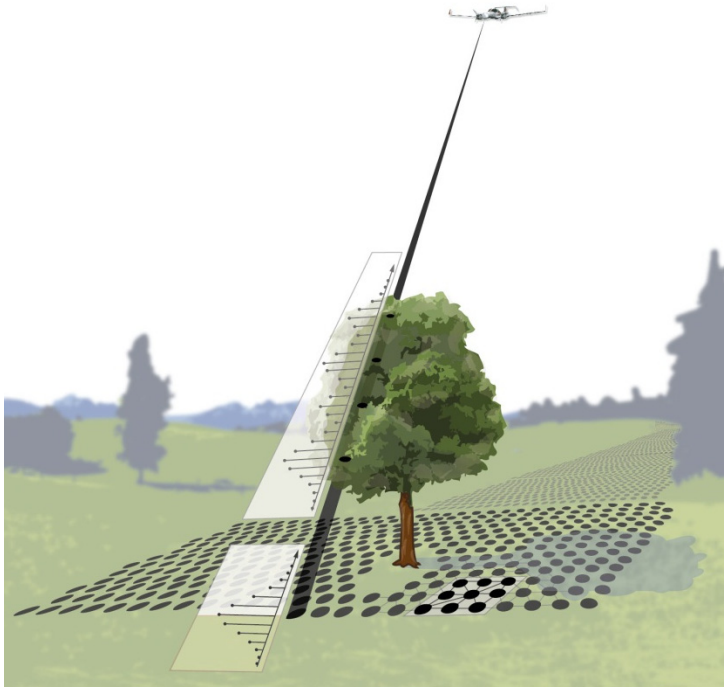

Figure 1: Sampling the environment with an echo digitizing sequentially scanning LIDAR instrument.

Figure 1 illustrates the sequential sampling by an airborne LIDAR system relying on a state-of-the-art LIDAR instrument with echo digitizing time-of-flight ranging and a rotating scan mirror, as described in detail in the sections to follow. The surface is sampled at the foot prints of laser pulses emitted at a high pulse repetition rate, typically about a few 100 000 pulses per second. The sequential sampling takes place in scan lines, shown in the illustration nearly perpendicular to the flight direction. In this example the sampling takes place from right to left within every line. In order to achieve an evenly

distribution of the sampling locations it is obvious that footprint spacing within the lines should be equal to the interline spacing.
The sampling in the third dimension, the height, is accomplished by sampling the echo signal originating from the interaction of the laser pulses with reflective objects, like the canopy of a tree and the terrain as shown in the example. For illustration we put the samples alongside the laser beam, i.e., the beam path of the short laser pulse although the actual sampling takes place in the LIDAR instrument. The sampling interval and the pulse width, more precisely the width of the instrument's system response determine the actual resolution in height (A. Ullrich, M. Pfennigbauer 2011).
There are some footprints highlighted: on the ground 9 footprints falling in a unit area hint at a property discussed later, the point density, usually measured in points per square meter. Some footprints in the foreground are interconnected by edges from a triangulation hinting to a second property discussed below, the point spacing or its inverse, the spatial sampling frequency. Additionally, some footprints along the measurement beam indicate targets derived from full waveform analysis allowing to precisely deriving ranges to nearly an unlimited number of targets per laser pulse, together with additional attributes for every detected target.
Requirements for airborne LIDAR surveys usually specify point density in points (or measurements) per square meter. However, this metric of points per square meter does not provide information about the actual spatial point distribution on the target area which constitutes the true quality of the data. In other words the value of the point density on a surface is only relevant together with information about the point distribution in two dimensions. A perfectly uniform point pattern will yield valuable sampling of the surface whereas an irregular point pattern produces inconsistent sampling and therefore the data provides less information, as will be demonstrated later.
Today's LIDAR marketplace offers a variety of airborne laser scanning (ALS) instruments with specification sheets that are often hard to read and to apply in real-world applications. The purpose of an ALS system is to capture the topography of the ground in an effective way by means of a large number of measured coordinates. Often the metrics of the specification sheets are given in terms of scanning rates and maximum operating altitudes, but these alone do not provide insight into the real productivity and quality of data produced by each instrument.
Additionally, the efficiency and productivity of ALS instruments is often assessed by the pulse repetition rate and scan speed of the system. While these metrics are helpful, they do not provide a complete or intuitive picture of the productivity achievable with such a system. Alternatively, the productivity and efficiency can be assessed by the total surface area the system can cover in a given period of time while ensuring a certain sampling quality. However, coverage speed and data quality, have not been addressed thoroughly in the past. We will attempt to answer the following questions:

1. How fast can LIDAR data be acquired while ensuring a specific point spacing on the ground?
2. How does height variation of terrain impact acquisition speed?
3. Can an instrument with lower maximum measurement rate outperform instruments with higher measurement rates with respect to total acquisition time?

2. POINT SPACING AND POINT DENSITY

LIDAR data – with the exception of data from flash LIDAR – is acquired sequentially, i.e., measurement by measurement in single laser output LIDAR instruments and two measurements at a time in dual laser output/dual channel instruments. In any case, when addressing point spacing, it is convenient to organize the actual measurements into scan lines. The whole scan pattern is then composed of a large number of scan lines. The measurements on the target surface have a spacing along the scan lines, we denote by *a*. The scan lines themselves have a specific spacing between each other, we denote by *b*. The distance of consecutive scan lines along the flight direction varies significantly over the swath width for oscillating scan mirrors, especially near the edges of the

swath, whereas the line spacing is almost constant over the swath width for rotating polygon scan mirrors.

It is common practice to base mission planning on either the nominal point spacing (NPS) or on the point density, usually measured in points per square meter (or similar points per area metrics). The "LIDAR Guidelines and Base Specification", (USGS 2010), states the term "nominal point spacing" without giving a rigorous definition of the term. The draft version of the ASPRS standard "LIDAR density and spacing specification", (ASPRS 2009), defines two metrics; the LDSS point spacing and the LDSS point density as statistical metrics for post-acquisition and post-processing quality control of ALS point clouds.

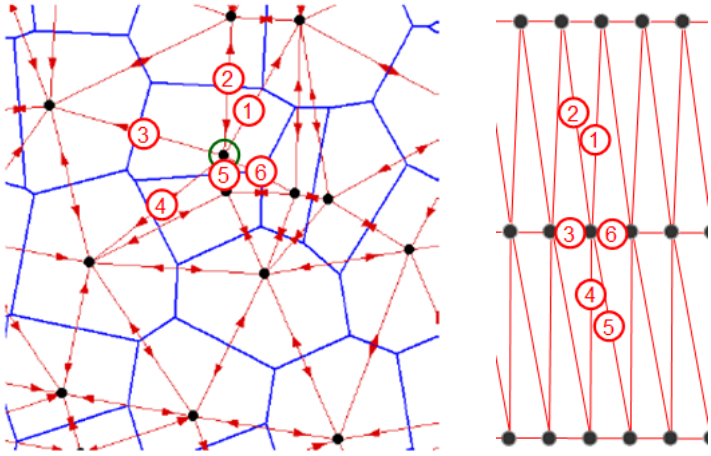

(a) (b)

Figure 2: Each black dot represents a measurement on the ground. The red lines are the edges of triangles according to a Delaunay triangulation. The blue polylines indicate Voronoi cells. Left: Irregularly distributed points. The example is taken from (ASPRS 2009). Right: Regular scan pattern with longer spacing between scan lines and shorter spacing along the scan lines.

The definition of point spacing is based on a Delaunay triangulation of the points on the ground. The draft proposes to attribute to each point a metric by taking the average length of all the edges connecting the specific point to all its neighboring points. However, for the subsequent considerations, we use a worst case nominal point spacing by taking the maximum of all edges instead of the average. This ensures that gaps in the sampling of the ground are accounted for and the metric is not reduced by very dense or even overlapping measurements within a single scan line, while having a wide line spacing (compare Figure 2).

In order to achieve some sort of symmetry between density and spacing metric, we will make use of the inverse of the nominal point spacing (1/NPS). Therefore we propose to use the two metrics:

Nominal sampling frequency, measured in points per meter, which is the inverse of the NPS. E.g., a sampling frequency of 2 points/m corresponds to a nominal maximum point spacing of 0.5 m.

Nominal point density, measured in points per square meter, i.e., the number of points within some test region, divided by the area of that region.

As it will be demonstrated further on, it is the nominal sampling frequency that actually determines the ability and quality in object detection, surface reconstruction, modeling and much more.

3. SCANNER DESIGN

Today all major commercial topographic ALS instruments rely on one of two scan mechanisms: a rotating multi-facet-mirror (i.e. polygon mirror), or an oscillating mirror. The clear advantage of using polygon mirrors is the continuous and smooth rotation of the mirror which leads to straight parallel scan lines on the ground (cf. Figure 3, a). The achievable scan rates are high and allow flexible adjustment for obtaining an even distribution of points on the ground. Furthermore, low vibrations and low stress on the deflecting mirror surfaces and the scan mechanism allow for maintaining constant and replicable measurement accuracy. The downside is that a certain fraction of the pulses produced by the laser do not result in actual measurements as they never leave the instrument.

This is contrasted by oscillating mirrors where all laser pulses are available for LIDAR measurements. Taking the movement of the platform into account, the resulting scan pattern on a flat ground is typically triangular or sinusoidal, depending on how the oscillator mirror is driven by the electronics. In general, the measurements on the ground tend to concentrate near the turning points of the mirror (Figure 3, b). By employing sophisticated scan control hard- and firmware this can be alleviated but never entirely overcome.
There is an emerging class of instruments making use of a single scan mechanism but employing two or even more rangefinders – or at least laser beams – which have optical axes slightly tilted with respect to each other as sketched in Figure 3, b. A third possibility is to use two facets of a rotating mirror to produce tilted scan lines as depicted in Figure 3, c. In every dual channel instruments, each channel has its own scan pattern on the ground. According to its design, there may be favorable or unfavorable interference pattern of the two scan patterns on the ground, especially on terrain with varying heights.

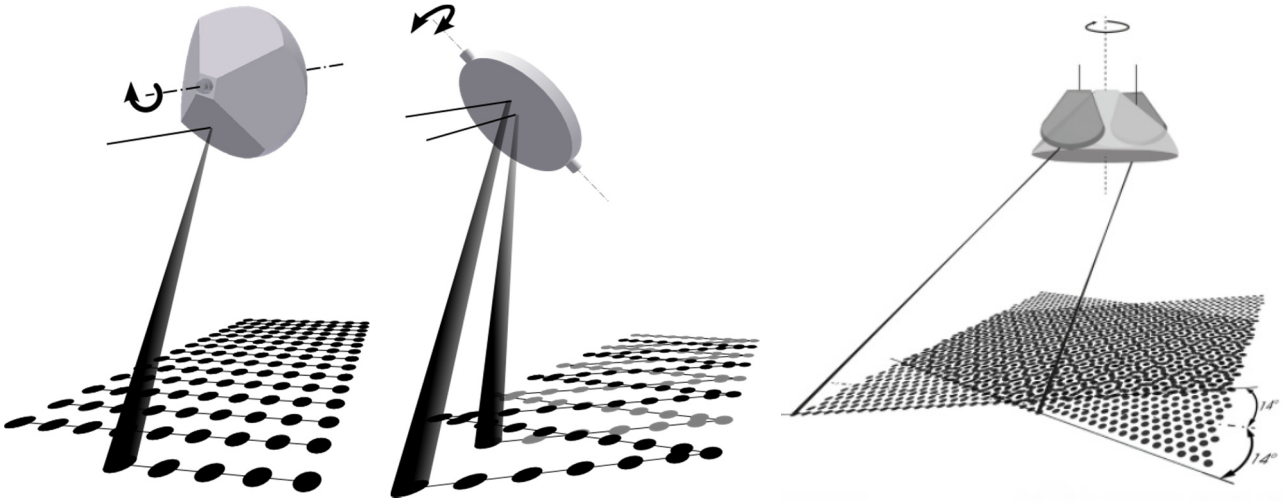

(a) (b) (c)

Figure 3: Principle of laser scanning mechanisms: (a) rotating polygon wheel with a single LIDAR channel, (b) oscillating mirror with a dual-channel LIDAR, (c) rotating polygon wheel with an innovative dual-channel design.

In the subsequent section scan patterns of dual channel instruments with an oscillating mirror and of single channel instruments with a rotating polygon mirror are discussed and compared in detail.

4. INSTRUMENT PERFORMANCE

Evaluating the impact of instrument parameters on the quality of the actual ground sampling we investigate point clouds derived by simulation. This is done for three state-of-the-art airborne laser scanning instruments with the parameters summarized in the table below (see web references)

	Instrument A	Instrument B	Instrument C
scan mechanism	rotating polygon	oscillating mirror	oscillating mirror
number of channels	single channel	dual laser output	dual laser output
flight altitude, AGL [1)]	50 m – 3000 m	150 m – 3500 m	150 m – 5000 m
laser pulse rate	100 kHz – 400 kHz	2 x 40 kHz – 2 x 250 kHz	2 x 50 kHz – 2 x 250 kHz
measurement rate	66 kHz – 266 kHz	80 kHz – 500 kHz	100 kHz – 500 kHz
pulses in the air	up to 12	2 x up to 2	not disclosed
field of view	0 deg – 60 deg	0 deg – 75 deg	0 deg – 75 deg
scan rate	10 LPS – 200 LPS	0 LPS – 2 x 200 LPS	0 LPS – 2 x 280 LPS

[1)] 10% target reflectance, 90% detection probability, 40 deg FOV, 23 km visibility

However, not all of the system parameters can be specified independently. In specific, there are two sets of parameters which are strongly related to each other: one set is field of view and scan rate, the other set is maximum permitted flight altitude (AGL), maximum laser pulse rate (measurement rate), and the capability of handling multiple pulses in the air.
The first set of parameters is discussed below when deriving the optimum number of lines per second for specific flight parameters. The second set is subsequently discussed in more detail by means of the so-called performance envelope.

4.1. Scanner performance

There is a significant interrelation between the field of view (FOV) and the number of scan lines per second for scanners with oscillating mirrors. For the further discussion we count a single scan line when the measuring beam moves from one edge of the swath to the other edge of the swath. We consider at first a single channel of the dual channel instruments and deal with the interference aspect later.
Figure 4 shows the dependencies of the maximum number of lines per second (maxLPS) and the maximum angular speed of the measuring beam (max$\partial\alpha/\partial t$) versus the field of view for the different instruments according to published specifications. It is worth noting that for Instrument A, both maxLPS and max$\partial\alpha\partial t$ are independent of FOV and high compared to the two other instruments at high FOV values.

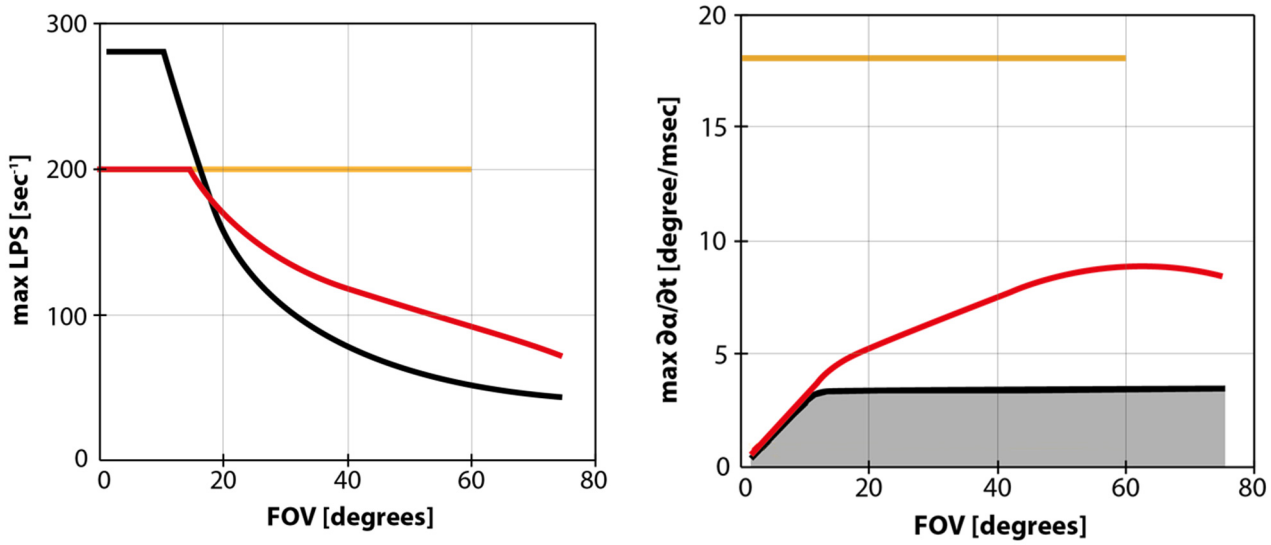

Figure 4: Left hand side: maximum number of lines per second (for a single channel) versus field of view (FOV) for Instrument A (orange), Instrument B with a sinusoidal scan pattern (red) and Instrument C with a triangular scan pattern (black). Right hand side: maximum angular speed of the laser beam versus FOV. Same coloring scheme used. The grey area indicates the possible choices of angular scan speed and FOV for Instrument C.

The number of lines per second translates directly into line spacing on the ground, *b*, and angular scan speed translates into point spacing within a scan line, *a*, as displayed in Figure 5. Given the speed above ground, *v,* of the LIDAR instrument, the line spacing *b* is simply $b=v/\text{LPS}$. The angular spacing between laser shots is simply $\partial\alpha/\partial t$ / PRR and the point spacing *a* on the ground for a given slant range R is $a=R\partial\alpha/\partial t$ / PRR.

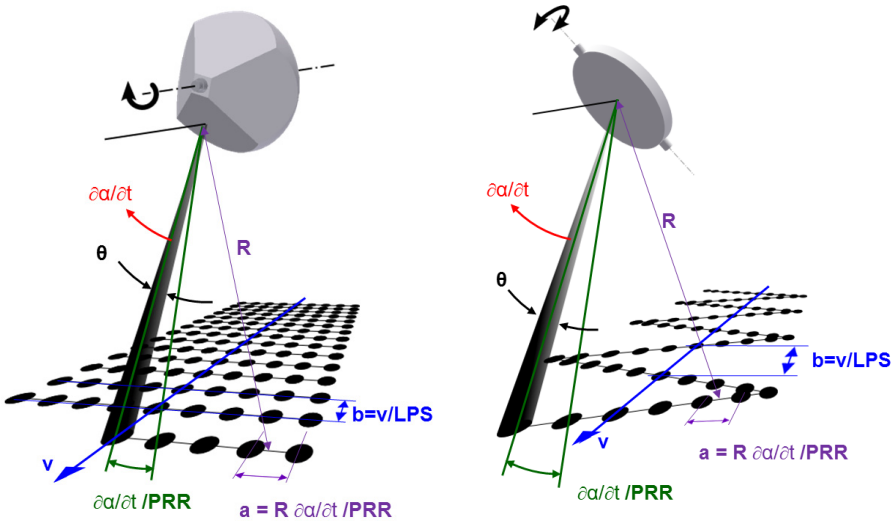

Figure 5: Point spacing within a scan line, a, and line spacing, b, on the ground for the polygon mirror scanner (left) and the oscillating mirror scanner (right). v ... speed of platform, LPS ... lines per second, PRR ... laser pulse repetition rate, ∂α/∂t ... angular speed of the measurement beam, θ ... beam divergence, R ... slant range.

In order to have non-overlapping laser footprints on the ground, Instrument B with a 1/e² beam divergence of 0.35 mrad would require a minimum angular speed of 5 degrees per millisecond for a PRR of 250 kHz (its maximum pulse repetition rate), but it is capable of providing 3 deg/msec maximum. Thus Instrument B cannot provide non-overlapping footprints and thus independent samples at its maximum PRR.

The high number of lines per second at low FOV seems favorable for some special applications. Unfortunately they do not translate into a high angular speed at low FOV as the mirror must stop at the edge of the FOV before accelerating into the opposite direction for each line. In the region where this reversed acceleration occurs, separating footprints on the ground becomes exceptionally difficult.

In order to achieve a high sampling frequency, it is common practice to try adjusting all parameters (AGL, speed above ground, PRR, LPS) in a way that the line spacing and the point spacing within the line become equal. Scan patterns are displayed in Figure 6 together with the equations for the optimum number of lines per second for each instrument. For the matrix scan pattern of Instrument A and the triangular scan pattern of Instrument C, the spacing *a*, at the edges of the swath must equal *b*, in the center of the swath. Whereas for the sinusoidal pattern of Instrument B, the spacing *a* is also taken at the center of the swath. For this calculation we already consider the optimum interference of the two scan patterns on the ground from the two channels of Instruments B and C, filling up the gaps at the edges of the swaths. Note that for the scan pattern of a single channel the line distance at the edges would be *2b*. Due to the low maximum scan speed of the oscillating mirror scanner for high FOVs, the optimum number of LPS according to the equations cannot be achieved for some parameter sets.

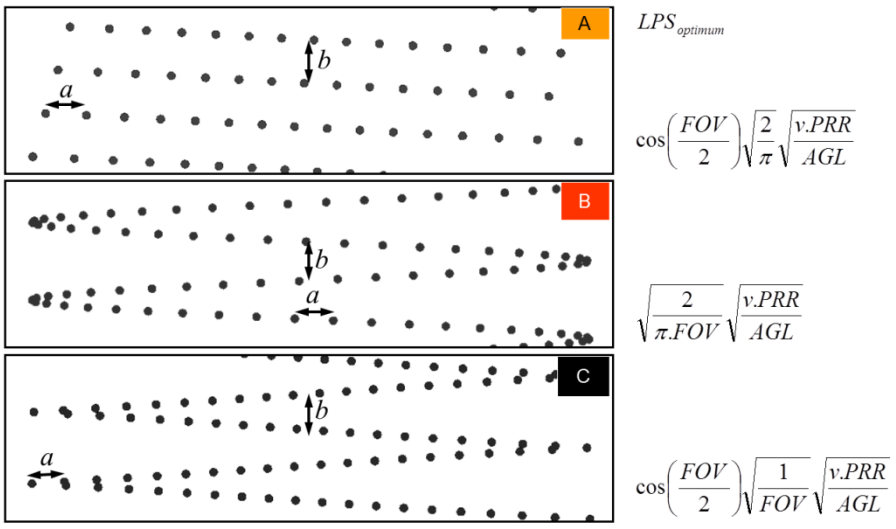

$$LPS_{optimum}$$

$$\cos\left(\frac{FOV}{2}\right)\sqrt{\frac{2}{\pi}}\sqrt{\frac{v.PRR}{AGL}}$$

$$\sqrt{\frac{2}{\pi.FOV}}\sqrt{\frac{v.PRR}{AGL}}$$

$$\cos\left(\frac{FOV}{2}\right)\sqrt{\frac{1}{FOV}}\sqrt{\frac{v.PRR}{AGL}}$$

Figure 6: Left: Scan pattern for Instrument A (top), and a single channel of Instruments B and C (middle and bottom) for illustration. Right: equations for the optimum choice of the number of lines per second. The equation for Instrument A is valid for a polygon mirror with four facets.

Instruments B and C perform range measurements in slightly different directions at the same time. As both channels are deflected by a single oscillating mirror, the two beams will be separated angularly in flight direction. Each channel generates its own scan pattern on the ground and it is the intention to have a favorable interference of the two scan patterns as sketched in Figure 7, top. The actual phase between the two scan patterns depends on the speed above ground, the height above ground, and the number of lines per second. For flat terrain, active control loops can ensure the favorable out-of-phase condition, whereas for mountainous terrain or even for hilly terrain, the phase condition cannot be maintained over the whole terrain and the favorable interference will develop into the unfavorable without the possibility of any counter measures.

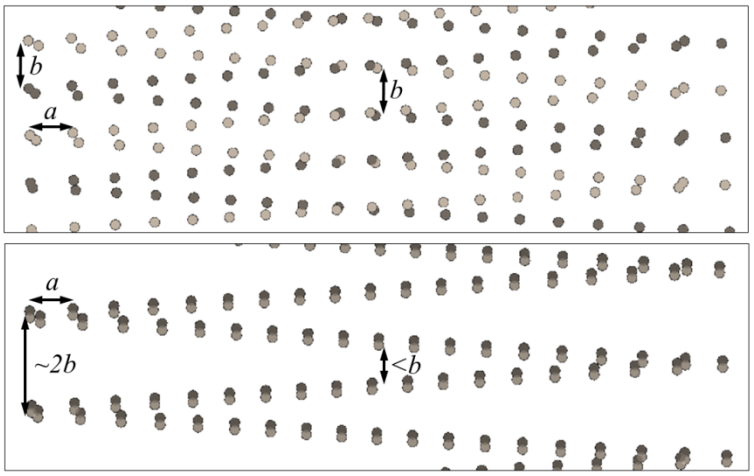

Figure 7: Interference patterns of instruments B and C. The scan patterns of the channels are shown in different shades of grey. Top: the favorable out-of-phase interference pattern. Bottom: the unfavorable in-phase interference pattern with *2b* line spacing at the edges.

4.2. Performance envelope

The performance envelope provides information on the maximum permitted pulse repetition rate for an intended flying height above ground for given target properties and atmospheric conditions. The performance envelopes displayed in Figure 8 are given for 40° FOV, 90% detection probability for 10% target reflectance, and 23 km visibility for the three instruments. The performance is directly related to the range finder of the LIDAR instrument and is thus given for a single channel for the dual channel instruments.

For example, Instrument A can be operated up to 2300 m AGL at a laser pulse rate (PRR) of 400 kHz. At higher altitudes the pulse energy of the laser pulses is too low to provide ranging to 10% reflectance targets. By lowering the PRR, the energy per pulse increases and ranging is feasible up to 3500 m AGL at a PRR of 100 kHz.

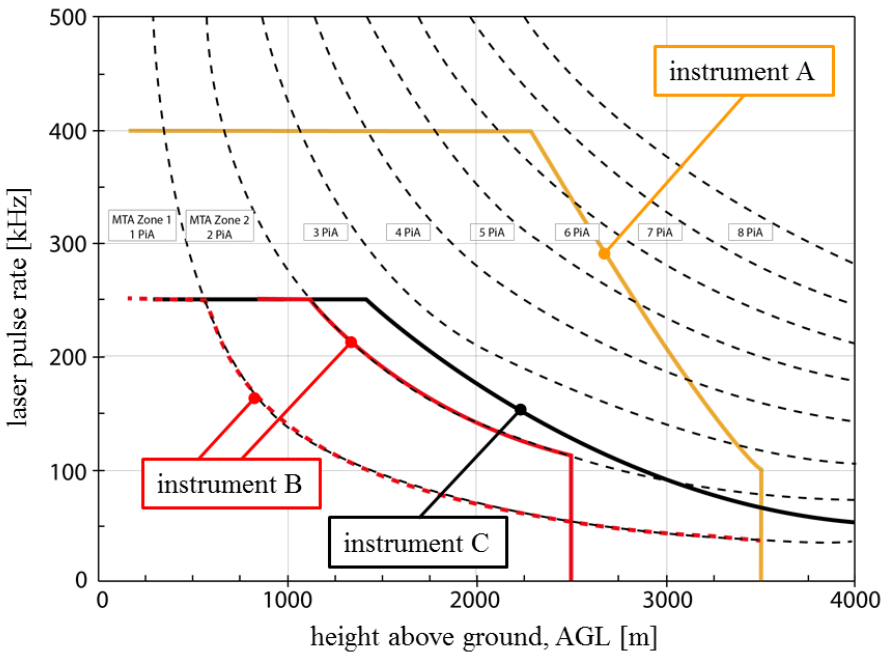

Figure 8: Performance envelope provided by the three instruments (per channel). Colors/styles used: orange Instrument A, red dashed Instrument B with just one pulse in the air, red solid Instrument B with 2 pulses in the air, black solid Instrument C. Dashed black lines indicate the borders of MTA zones.

The performance envelope clearly shows the benefit of handling a large number of pulses in the air simultaneously. This capability enables Instrument A to fully exploit its high potential of acquiring data *fast* from *high altitudes*. Additionally, instrument A is capable of acquiring data in different MTA (multiple time around) zones within a single flight swath (P. Rieger, A. Ullrich 2012). In contrast, for Instrument B and C, proper flight planning must ensure that all targets at least within a single scan line of a swath will safely remain in one single MTA zone (compare Figure 9).

.

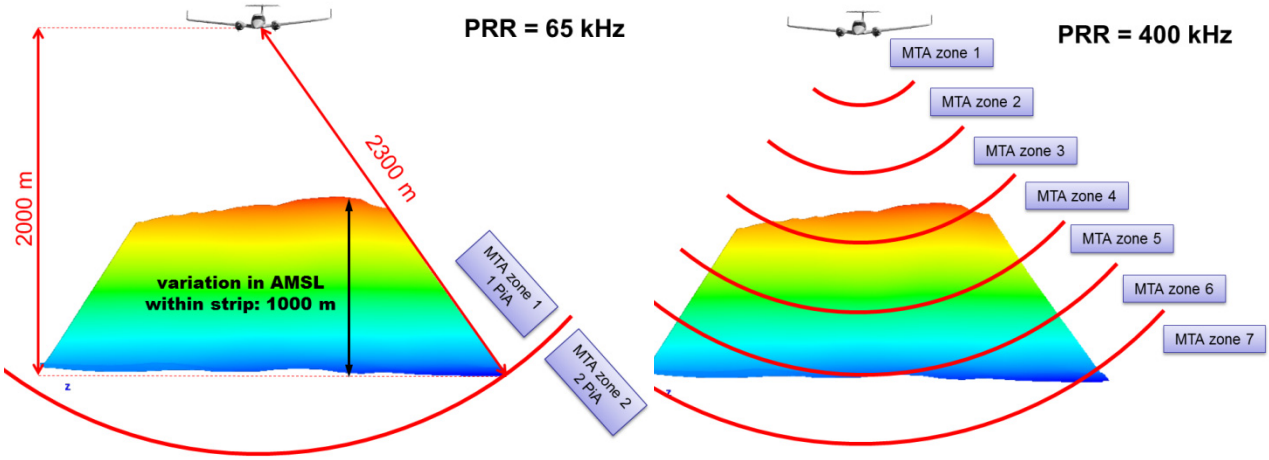

Figure 9: Illustrating multiple pulses in the air and its impact on the maximum permitted laser pulse repetition rate. Left: in order to ensure that all targets of flight swath over mountainous terrain with 1000 m height variation remain in a single MTA zone, the PRR must be limited to 65 kHz. Right: Instrument A can acquire data simultaneously in more than a single MTA zone. In the example shown, data are acquired in zones 3 through 7.

5. PERFORMANCE COMPARISON

Subsequently we analyze the point density, point spacing, and point distribution under typical surveying conditions in a challenging scenario, i.e., data acquisition in a mountainous region, for the three instruments A to C. Assuming a straight flight line with a speed above ground of 140 kn, the height above ground (AGL) varies between 1000 m and 2000 m. Figure 10 provides a view of the terrain model used for the simulation.

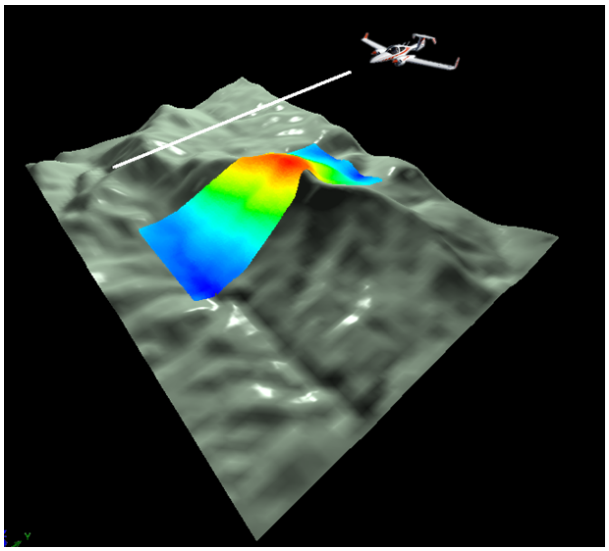

Figure 10: Terrain model used for simulation. Height encoded point cloud of Instrument A overlaid.

Acquiring LIDAR data in a mountainous region is, in general, a challenging task. A common approach in providing high density LIDAR data in mountainous regions is to work with rather small swath widths and to follow the terrain. However, this reduces the acquisition speed measured in km²/h drastically and thus makes the data acquisition considerably more expensive.

With Instrument A's ability to acquire data in different MTA zones within a single swath enables an alternative approach: flying high with a fixed wing aircraft. This yields the most time-efficient and cost efficient approach.

The subsequent simulation reflects this approach. Flying at AGL values between 1000 m and 2000

m above the terrain (1000 m height variation of the terrain) without attempting to follow the ground produces point clouds with significantly different sampling qualities for the three instruments.
Mountainous terrain as well hilly terrain is especially challenging for instruments B and C as the intended out-of-phase condition for the scan patterns of the two channels cannot be maintained due to the significant change in AGL, even in a single scan line.
Furthermore, the pulse repetition rate and thus the measurement rate of Instruments B and C have to be reduced significantly to ensure that all objects are within a single MTA zone.
The table below summarizes the achievable point spacing and Figure 11 shows the distributions of the laser footprints in nadir and at the swath edges. Note that for the swath edges two different distributions are displayed. The best case reflects the favorable out-of-phase interference, whereas the worst case reflects the unfavorable but unavoidable in-phase condition.

	AGL	FOV	measurement rate	LPS	point spacing *a*	line spacing *b*	avg. point density
Instrument A	2000 m	60 deg	1x 266 kHz	1x 83 LPS	0.87 m	0.87 m	1.3 – 3.5 p/m²
Instrument B	2000 m	60 deg	2x 63 kHz	2x 37 LPS	1.94 m	4.32 m	0.53 – 1.9 p/m²
Instrument C	2000 m	60 deg	2x 66 kHz	2x 41 LPS	1.74 m	3.50 m	0.9 – 2.6 p/m²

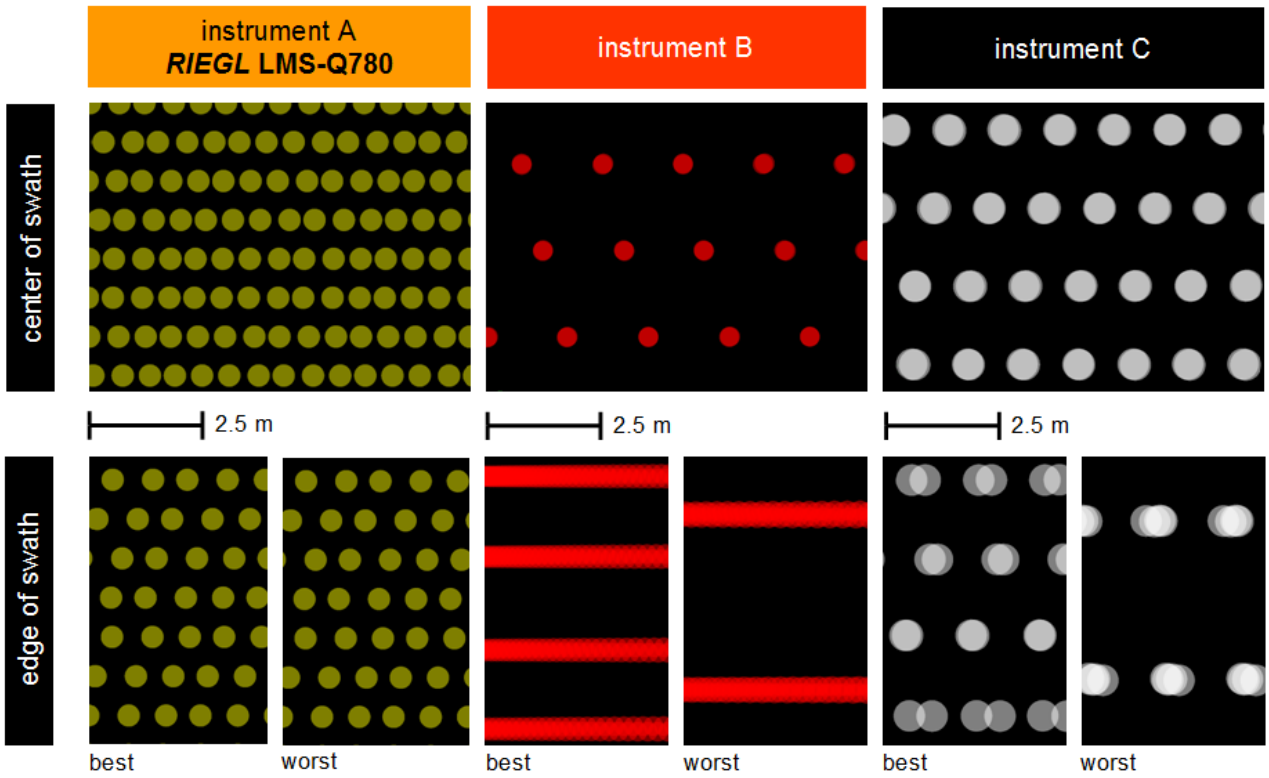

Figure 11: Distribution of laser footprints derived by parameter optimization and by simulation on mountainous terrain.

6. SAMPLING WITH LASER FOOTPRINTS

In order to demonstrate the crucial importance of the nominal point spacing and thus the sampling frequency of a specific scan pattern we placed a simulated artificial object on the mountainous terrain near the edge of the swaths generated for every instrument. To make the reader familiar with the display, a real example is shown in Figure 12 below showing a point cloud, color encoded by height, from a top view. Blue footprints hit the lower surroundings of a small house, whereas the red footprints are located on the roof. The object becomes more easily recognized when taking perspective views on the point cloud.

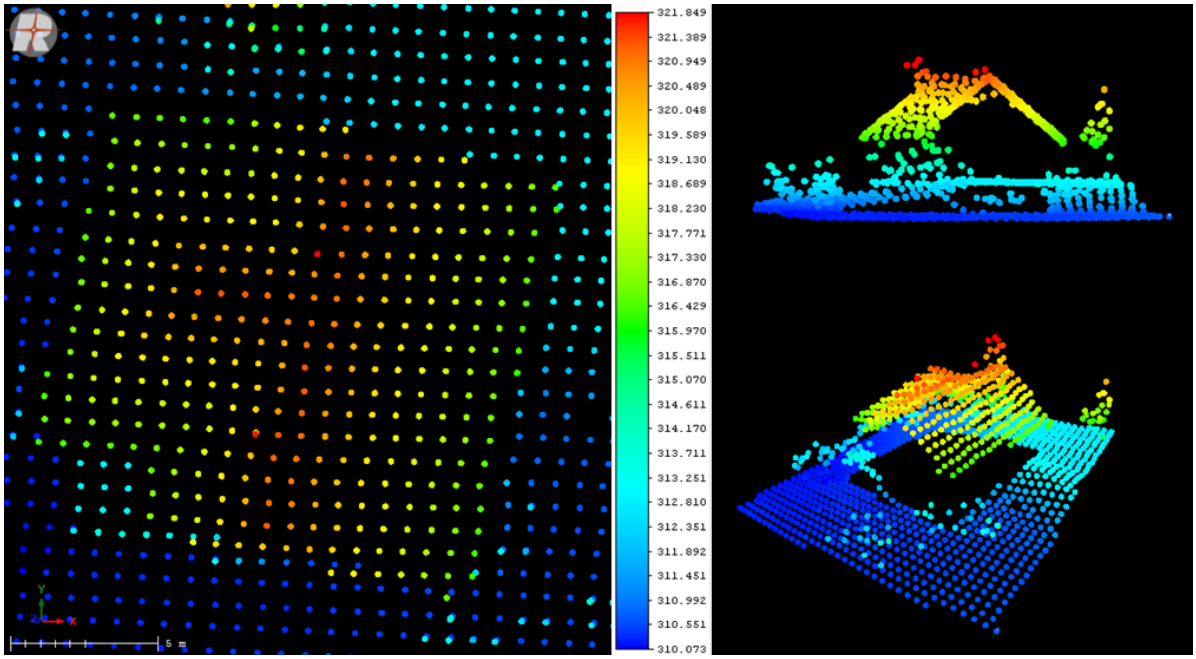

Figure 12: Real world example of an object sampled with Instrument A. Left: top view of point cloud, Color encoding according to height (blue .. low, red .. high). Right: perspective views of the same point cloud.

Figure 13 shows simulated point clouds on the artificial object. Color encoding is similar to the one used in Figure 12: a laser footprint is colored blue when hitting a low target surface, red when it hits an elevated target surface. According to the sampling theorem, the sampling frequency must be at least twice the highest spatial frequency of the object to be sampled, in order to be able to reconstruct the object or at least to do an object recognition/detection routine. Even though the point density measured in points per square meter is more or less the same for all of the instruments, the sampling quality is tremendously different. The artificial objet – the writing "PHOWO" can be clearly recognized in the point cloud from Instrument A, whereas not even guessing from the point clouds from Instruments B and C would reveal the nature of the object.

7. ACQUISITION SPEED

In order to answer the question, "How fast can LIDAR data be acquired with a specific instrument while ensuring a specific sampling quality?", we provide below a plot of the sampling frequency in points/meter, i.e., the inverse of the nominal point spacing versus the acquisition speed. Acquisition speed is simply calculated as the product of ground speed and swath width. Acquisition speed is usually stated in the unit of square kilometers per hour and reflects the area covered by a single swath, not taking into account the commonly used overlap of swaths. For Instruments B and C we follow the common practice of discarding all measurements lying near the edges of the swath (i.e. near the turning points of the oscillating mirror) according to the manufacturers' recommendations.

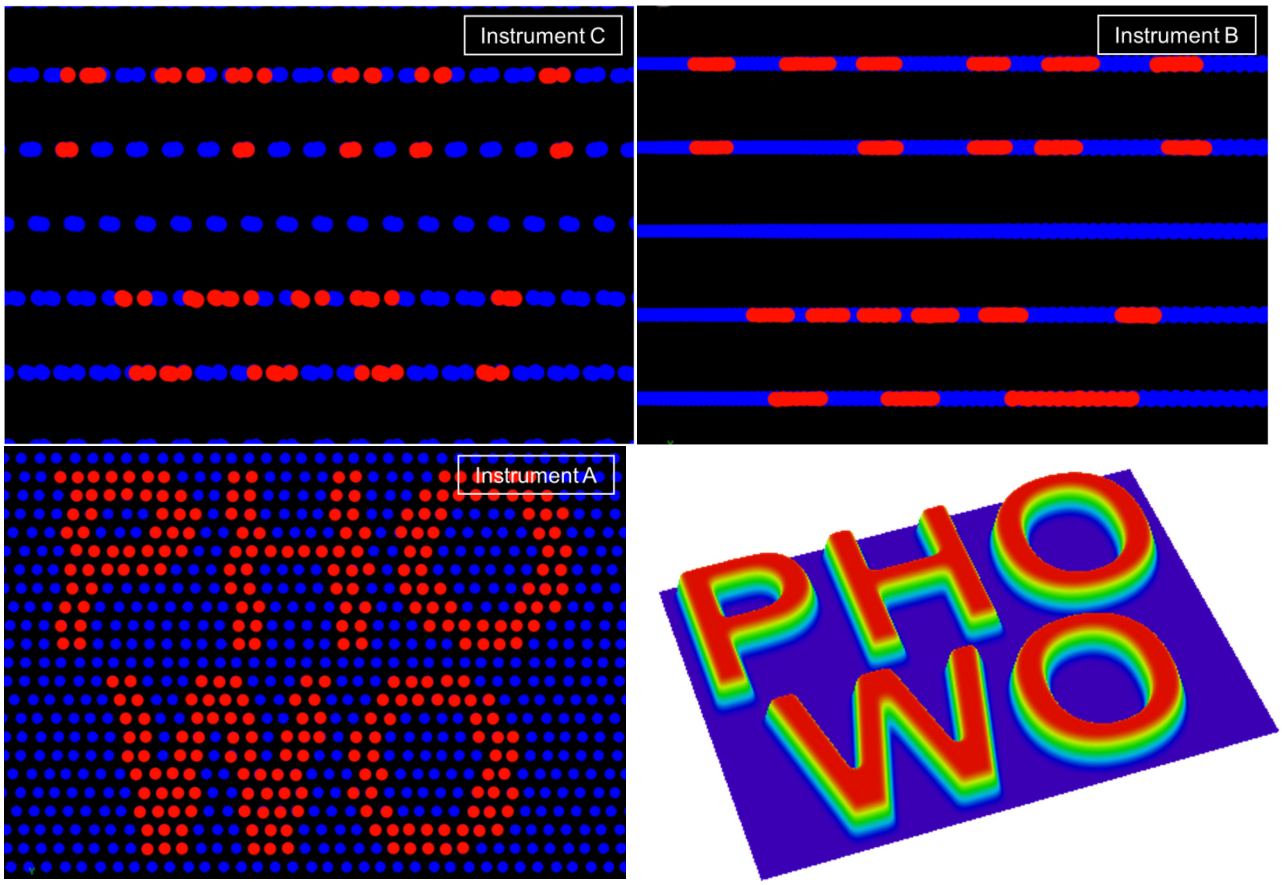

Figure 13: Sampling an artificial object (bottom right) by simulated point clouds. Red indicated footprints on higher elevation compared to blue footprints hitting lower elevation objects. Black indicated areas not sampled. Top left: sampling by instrument C. Top right: sampling by instrument B. Bottom left: sampling by instrument A.

Figure 14, left, shows such a diagram for instrument A. For example, if a sampling frequency over the full swath width of at least 4 measurements per meter (nominal point spacing of better than 0.25 m) must be achieved, the maximum acquisition speed is 33 km² per hour. The same acquisition speed can be achieved from different heights and different speeds with instrument A within a wide range allowing to adapt to the abilities of the aircraft used. The diagram also reflects the general trend, that acquiring data with a high sampling frequency (low nominal point spacing) asks for a low acquisition speed.

Figure 14, right, we show the performance as sampling frequency versus acquisition speed for Instrument A and B on flat terrain. For the sake of clarity we do not include the performance of Instrument C in the subsequent diagrams, which is slightly worse than that of instrument B.

In the region from 20 km²/h to 200 km²/h, the difference between Instrument A and B is small. Nevertheless, the 266,000-measurements-per-second system outperforms the 500,000-measurements-per-second system by providing 10% better point spacing or a 20% faster data acquisition. Acquisition speeds above 200 km²/h call for acquisitions from higher AGLs, which reduces the maximum permitted laser pulse repetition rate for Instrument B as it can only acquire data in a single MTA zone and thus reduces the sampling frequency and acquisition speed even further compared to instrument A. Instrument A outperforms Instrument B in the regime of 600 km²/h by 60% in point spacing and a factor of 2 in acquisition speed. On the left hand side of the diagram, at very high sampling frequencies (more than 4 per meter) the limitations by the oscillating mirror scanner increase the gap in performance in favor of instrument A.

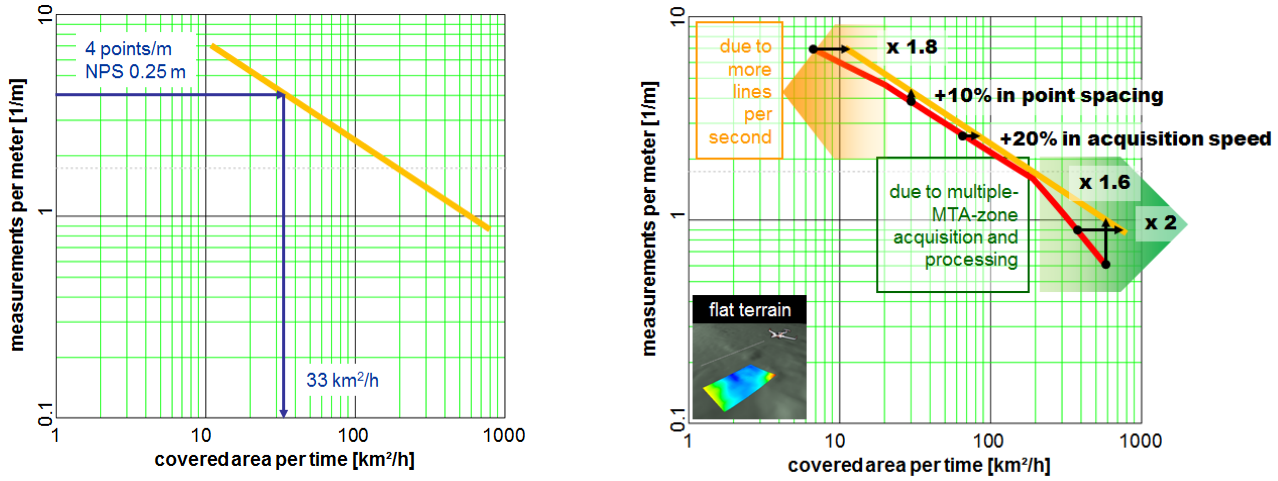

Figure 14: Sampling frequency versus acquisition speed. Left: for Instrument A. Right: for instruments A (orange) and B (red) for data acquisition on flat terrain.

For hilly terrain with an assumed variation in height above mean sea level of 200 m and thus AGL within a single strip, the out-of-phase condition between the two channels of Instrument B and C cannot be maintained over the full swath and thus parameters must be optimized differently compared to what has been stated in section 4.1. ($a = b/2$ instead of $a = b$). Figure 15, left, shows the achievable performance. The difference is now much larger. Even for medium acquisition speeds (20 km²/h to 200 km²/h), data acquisition with Instrument A is 2.6 times faster than Instrument B. Or, for the same acquisition speed, Instrument A provides 60% better sampling frequency.

For mountainous terrain with an assumed variation in height above ground of 1000 m within a single strip, once more the out-of-phase condition between the two channels of Instrument B and C cannot be maintained over the full swath. Additionally, the restriction that Instrument B can acquire data only in a single preselected MTA zone reduces the permitted laser pulse repetition rate drastically. Figure 15, right, shows significant difference, both in acquisition speed and in sampling frequency. Even for medium acquisition speeds (20 km²/h to 200 km²/h), data can be acquired with Instrument A 8 times faster compared to instrument B. Or, for the same acquisition speed, Instrument A will haves 170 % better sampling frequency.

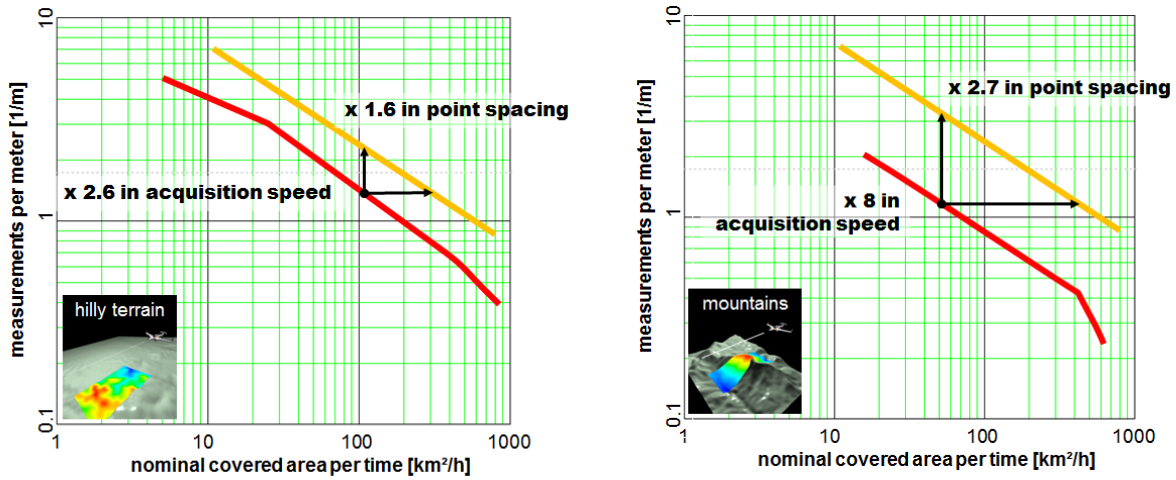

Figure 15: Sampling frequency versus acquisition speed for instruments A (orange) and B (red) for data acquisition on hilly terrain (left) and mountainous terrain (right).

8. SUMMARY

Information from airborne LIDAR data on terrain, vegetation, man-made and natural objects is captured by taking spatial samples. The spatial resolution is fundamentally limited by the bandwidth/system response of the time of flight rangefinder along the laser beam path and by the footprint diameter/beam profile of the laser footprints across the beam path. However, these fundamental limits are usually not reached in LIDAR data acquisitions, as the footprint spacing exceeds the footprint diameter in most real world scenarios.
The way the actual footprints are distributed on the objects has a crucial impact on how well information can be extracted from the resulting point clouds and how well objects can be recognized. We have demonstrated that LIDAR instruments relying on rotating polygon mirrors for beam deflection, with the capability of acquiring data regardless of how many emitted pulses are simultaneously in the air clearly outperforms other LIDAR instruments even providing more measurements on the ground per second.

9. REFERENCES

ASPRS (2009), ASPRS Standard Version 1.0, Draft 2, “LIDAR density and spacing specification”.

Naus, T. (2008), “Unbiased LIDAR Data Measurements (Draft)”.

Rieger, P., Ullrich, A. (2012), “Resolving range ambiguities in high-repetition rate airborne light detection and ranging applications”. J. Appl. Remote Sens. 6(1).

Ullrich, A., Pfennigbauer, M. (2011), “Echo Digitization and Waveform Analysis in Airborne and Terrestrial Laser Scanning”. Proceedings of the 53rd Photogrammtric Week, September 2011, Stuttgart.

Ullrich, A., Pfennigbauer, M., Rieger, P. (2013), “How to read your LIDAR spec – a comparison of single-laser-output and multi-laser-output LIDAR instruments”. ILMF 2013.

USGS (2010), U.S. Geological Survey, National Geospatial Program, “LIDAR Guidelines and Base Specification”, Version 13.

www:
http://www.geo-matching.com
http://www.riegl.com